Dehydration in the Arctic stratosphere during the SOLVE/THESEO-2000 campaigns

C. Schiller,[1] R. Bauer,[1] F. Cairo,[2] T. Deshler,[3] A. Dörnbrack,[4] J. Elkins,[5] A. Engel,[6] H. Flentje,[4] N. Larsen,[7] I. Levin,[8] M. Müller,[6] S. Oltmans,[5] H. Ovarlez,[9] J. Ovarlez,[9] J. Schreiner,[10] F. Stroh,[1] C. Voigt,[4] and H. Vömel[5]

Received 2 February 2001; revised 5 July 2001; accepted 9 July 2001; published 22 October 2002.

[1] Balloon-borne measurements of H_2O, CH_4, and H_2 in January and March 2000 show clear evidence for dehydration inside the polar vortex. At 30–50 hPa, total hydrogen is reduced by approximately 0.5 ppmv. This phenomenon is apparent in all five in situ balloon observations of this period; therefore it is probable that dehydration occurred over extended regions and a long period of this winter which was characterized by a well-confined vortex and low stratospheric temperatures. At altitudes below 50 hPa, where dehydration was strongest in previous Arctic observations and in the austral spring, total hydrogen values ($2 \cdot CH_4 + H_2O + H_2$) were similar to those found in Arctic profiles from other years where there was no dehydration and to those found at midlatitudes. In some of the dehydrated air masses, small solid particles were found whose crystallization might be connected to the earlier formation of ice particles. Back trajectory calculations for the January observations indicate that the probed air masses had experienced temperatures below the ice frost point in a synoptic-scale cold region several days before the observations. Most likely, the air was dehydrated there. In addition, temperatures in these air masses dropped below ice saturation several hours prior to the observations in the lee of the Scandinavian mountain ridge. For the March measurements, no ice saturation was apparent in the recent history of the air masses, again indicating that dehydration in the Arctic winter 1999/2000 was not a local phenomenon. *INDEX TERMS:* 0340 Atmospheric Composition and Structure: Middle atmosphere—composition and chemistry; 0305 Atmospheric Composition and Structure: Aerosols and particles (0345, 4801); 9315 Information Related to Geographic Region: Arctic region; *KEYWORDS:* Water vapor, total hydrogen, Arctic stratosphere, dehydration

Citation: Schiller, C., et al., Dehydration in the Arctic stratosphere during the SOLVE/THESEO-2000 campaigns, *J. Geophys. Res.*, *107*(D20), 8293, doi:10.1029/2001JD000463, 2002.

1. Introduction

[2] Dehydration of the lower stratosphere during the polar winter, resulting from the formation and subsequent sedimentation of polar stratospheric clouds (PSC), was first reported for the Antarctic vortex by *Kelly et al.* [1989], based on airborne measurements. In the following years, the spatial extent and the temporal development of this phenomenon over the Austral winter and spring period has been investigated both from balloon soundings [*Vömel et al.*, 1995] and from satellites [*Nedoluha et al.*, 2000]. The most severe H_2O removal down to minimum values of 2 ppmv was observed at altitudes from 12 to 21 km, beginning in June/July and persisting for several months until November.

[3] In the Arctic winter, however, dehydration is much less frequent and, if occurring, less severe. The majority of data from the Arctic do not show dehydration inside the vortex [e.g., *Kelly et al.*, 1990; *Engel et al.*, 1996; *Randel et al.*, 1998]. So far, dehydration in the Northern Hemisphere has been documented for single events only, which were observed during the cold winters of 1988/1989 [*Fahey et al.*, 1990], 1994/1995 [*Stowasser et al.*, 1999; *Ovarlez and Ovarlez*, 1995] and 1995/1996 [*Vömel et al.*, 1997; *Hintsa et al.*, 1998]. These winters were characterized by very low temperatures during December and January [*Pawson and Naujokat*, 1999]. All authors report a moderate dehydration in layers between 16 and 20 km altitudes, with the exception of *Vömel et al.* [1997], who found a layer between 20 and 23

[1]Forschungszentrum Jülich, Institut für Chemie und Dynamik der Geosphäre I, Jülich, Germany.
[2]Instituto di Fisica dell'Atmosfera - Consiglio Nazionale delle Ricerche, Rome, Italy.
[3]Department of Atmospheric Sciences, University of Wyoming, Laramie, WY, USA.
[4]Deutsches Zentrum für Luft- und Raumfahrt, Institut für Physik der Atmosphäre, Wessling, Germany.
[5]Climate Monitoring and Diagnostics Laboratory, NOAA, Boulder, Colorado, USA.
[6]J. W. Goethe Universität Frankfurt, Institut für Meteorologie und Geophysik, Frankfurt, Germany.
[7]Danish Meteorological Institute, Copenhagen, Denmark.
[8]Institut für Umweltphysik, Universität Heidelberg, Heidelberg, Germany.
[9]CNRS, Laboratoire de Météorologie Dynamique, Palaiseau, France.
[10]Max-Planck-Institut für Kernphysik, Heidelberg, Germany.

0148-0227/02/2001JD000463$09.00

km altitude, showing water vapor mixing ratios as low as 3 ppmv.

[4] The interpretation of low values of water vapor in the polar winter stratosphere is ambiguous, in particular when the observed effect is small. They can either be caused by dynamical processes (e.g., transport of drier air from mid-latitudes) or by removal of water vapor from the gas phase. Therefore it is necessary to observe long-lived tracers simultaneously with water. The most appropriate tracers to measure simultaneously are methane (CH_4) and molecular hydrogen (H_2). These species, together with water, are photochemically coupled and by far the most abundant hydrogen-containing species in the stratosphere. Thus total hydrogen ($2{\cdot}CH_4 + H_2O + H_2$) and to some extent also the quantity $2{\cdot}CH_4 + H_2O$ is expected to be constant in the absence of dehydration and in air masses which are far enough from the tropical source regions and high enough not to be influenced by seasonal cycles in the input of water vapor from the troposphere into the stratosphere. For example, *Schmidt and Khedim* [1991] found that there is no seasonal cycle of CO_2 left in Arctic vortex air masses with pressure less than 80 hPa. The following studies are therefore restricted to altitudes above this level.

[5] Further, depending on the lifetime of water-containing particles and their size, the removal of water vapor from the gas phase can be either a reversible phenomenon or an irreversible one if the particles live long enough to fall and remove water vapor permanently from an air mass. For the investigation of dehydration, which is generally defined as irreversible removal, it is thus desirable to measure total water, which includes both gas phase and particle bound H_2O.

2. Observations and Analysis

2.1. Experiments

[6] Here data from SOLVE/THESEO-2000 balloon-borne measurements carried out in early 2000 from Kiruna, Sweden (68°N, 21°E), are reported. The balloon flights used in this study are listed in Table 1.

[7] On both flights of the so-called Triple payload, H_2O was measured using the Jülich fast in situ stratospheric hygrometer (FISH) which is based on the Lyman α photofragment fluorescence technique. Technical details and the calibration procedure are given by *Zöger et al.* [1999]. The hygrometer measures the total water content, that is, H_2O in the gas and in the condensed phase, since particles are sampled as well and then evaporated in the heated inlet tube. In the stratosphere the precision of a 1 s measurement is 0.15 ppmv, and the overall accuracy is 5%. In order to avoid potential contamination artifacts, only data at definite descent rates > 2 m s^{-1} are evaluated.

[8] The Triple payload further includes a whole air sampler [*Schmidt et al.*, 1987] to measure vertical profiles of long-lived tracers, among others those of CH_4 and H_2. The precision of the CH_4 measurement is better than 0.2%, the total accuracy better than 1.2%. For H_2 the precision is better than 2% and the total accuracy better than 4%. In addition, a chemical conversion resonance fluorescence instrument to measure the ClO/BrO concentration (for data obtained with this instrument see *Vogel et al.* [2002]) and optical particle counters were operated on this payload. On 27 January, the Laboratoire de Météorologie Dynamique (LMD) laser diode particle counter [*Ovarlez and Ovarlez*, 1995] was used, and on 1 March the backscatter sonde LABS [*Adriani et al.*, 1998] was used.

Table 1. Balloon Flights and Payload Composition During the SOLVE/THESEO-2000 Winter Used in This Study

Date	H_2O	CH_4	$2{\cdot}CH_4 + H_2O$, ppmv	Payload/ Reference
19 January 2000	LMD	n.d.	n.d.	PSC analysis
27 Jan 00	FISH	cryosampler	7.0 ± 0.15[a]	Triple
27 Jan 00	NOAA	(Triple)	n.d.	2 hours after Triple
01 Mar 00	FISH	cryosampler	7.0 ± 0.15[a]	Triple
05 Mar 00	NOAA	LACE/OMS	n.d.	5.5 hours after OMS
1991/1992	LMD	cryosampler	6.91 ± 0.41	*Engel et al.* [1996]
11 Feb 97	FISH	cryosampler	7.02 ± 0.11	Triple
06 Feb 99	FISH	cryosampler	7.05 ± 0.12	Triple

In the second half of the table, additional flights from previous winters that are used for comparison are listed. All balloons were launched at 68°N. The errors given for $2{\cdot}CH_4 + H_2O$ represent the variability (standard deviation) and do not include the accuracy of the measurements.

[a] Data in dehydrated layers are not considered.

[9] Further, several flights of the National Oceanic and Atmospheric Administration (NOAA) frost point hygrometer [*Oltmans*, 1985] were carried out during this winter of which only those obtained in the year 2000 are considered in the following. On 27 January, the hygrometer was launched 2 hours after the Triple payload, so that tracer measurements from the cryosampler can be used. On 5 March, tracer information can be obtained from the LACE experiment [*Ray et al.*, 1999] on board the OMS payload which was launched 5.5 hours prior to the hygrometer.

[10] In addition, H_2O data from one balloon flight of the so-called PSC analysis payload on 19 January using the LMD frostpoint hygrometer [*Ovarlez and Ovarlez*, 1994, 1995] are presented. For this day, no tracer measurements are available.

2.2. Hydrogen Species

[11] The five H_2O profiles measured during SOLVE/THESEO-2000 are plotted in Figure 1. The slope of the profiles is different, depending on the degree of subsidence inside the polar vortex. The profiles on 19 and 27 January show approximately the same slope which is larger than for measurements at midlatitudes; the profiles were measured inside the polar vortex (e.g., 27 January, potential vorticity (PV) = 70–80 PVU at θ = 500 K and PV = 110–120 PVU at θ = 550 K; 1 PVU = 10^{-6} K m^2 kg^{-1} s^{-1}). On 1 March, the slope of the H_2O profile is even larger; the measurements were carried out deep inside the polar vortex (PV > 80 PVU at θ = 500 K and PV > 120 PVU at θ = 550 K) and are comparable to those with strongest gradients observed in previous years [*de La Noë et al.*, 1999].

[12] The descent of the Triple balloon on 27 January and 1 March occurred at a rate of 2–5 m s^{-1} and included a float of a few hours at approximately 35 hPa, primarily planned for photochemical studies. During this float or generally at descent rates slower than 2 m s^{-1}, part of the H_2O data are obviously contaminated as known from previous flights [*Schiller et al.*, 2001]. When discussing dehydration events in the following, the analysis is based on the data observed just before the float altitude is reached and

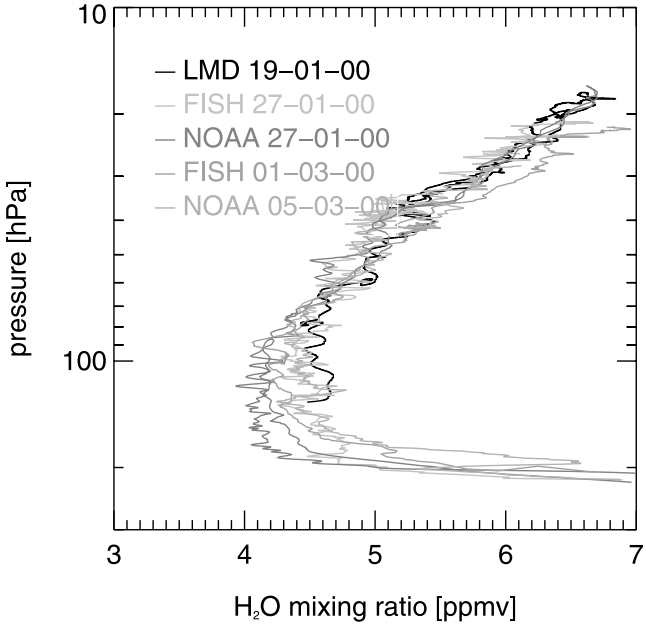

Figure 1. H_2O profiles measured during SOLVE/THESEO-2000 on 19 January, 27 January, 1 March, and 5 March 2000. See color version of this figure at back of this issue.

which are amongst the lowest H_2O mixing ratios at these altitudes. For the following data during the float, the lower envelope of the data still shows an irregular variability between the minimum value at the beginning of the float and a value that is higher by approximately 0.5 ppmv. It is not clear whether a remaining contamination artifact or horizontal variability of the atmospheric H_2O distribution is the reason for these observations.

[13] On 27 January, the NOAA frost point hygrometer measured a H_2O profile that shows the same layer with low water as the Triple payload on the same day (Figure 1). Note the excellent agreement between FISH and the NOAA frost point hygrometer measurements both in absolute values and the observation of small-scale features (K. H. Rosenlof et al., Intercomparison of hygrometers during SOLVE/THESEO-2000, manuscript in preparation, 2001). The profile data of this hygrometer obtained on 5 March show a region at 50–30 hPa where water vapor does not increase further or exhibits layers of even slightly lower mixing ratios than the ambient 5.5 ppmv.

[14] For the flights on 27 January, 1 March, and 5 March, when simultaneous tracer measurements are available, Figures 2a–2c show the mixing ratio profiles of H_2O, CH_4, H_2, and of the derived quantities $2{\cdot}CH_4 + H_2O$ and total hydrogen = $2{\cdot}CH_4 + H_2 + H_2O$. For comparison, also $2{\cdot}CH_4 + H_2O$ and total hydrogen data of the Triple payload from previous years are indicated by red lines. As mentioned before, only data from well-mixed air masses above a pressure altitude of 80 hPa will be considered in order to exclude possible seasonal or regional variability of the total water content in the lowermost stratosphere. For the 3 days, $2{\cdot}CH_4 + H_2O$ is significantly, that is, by ≈ 0.5 ppmv lower in the altitude region around 40 hPa ($\theta \approx 500$ K) than at altitudes above and below. On 1 March, the lower boundary

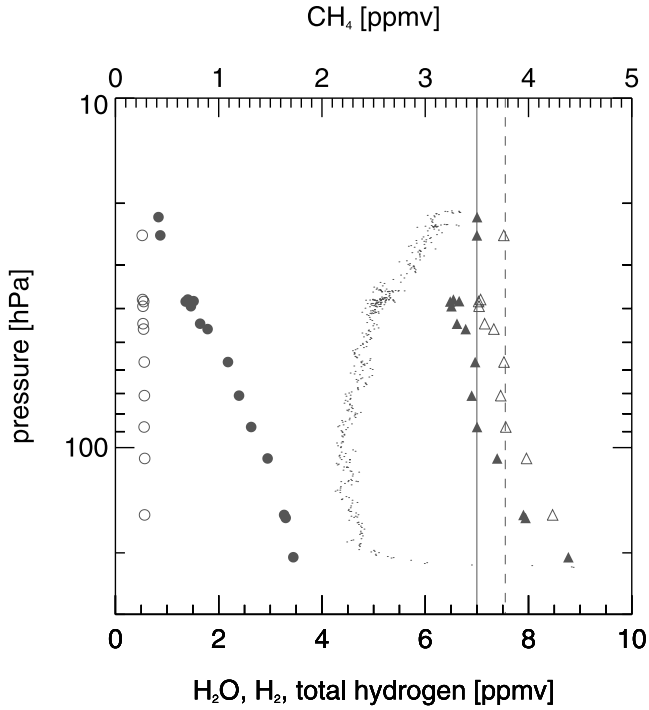

Figure 2a. Partitioning of hydrogen species for the Triple flight on 27 January 2000. Open circles, H_2; solid circles, CH_4; dots, H_2O; solid triangles, $2CH_4 + H_2O$; open triangles, total hydrogen. Vertical lines denote mean values of $2CH_4 + H_2O$ (solid line) and total hydrogen (dashed line), respectively, derived from previous winters.

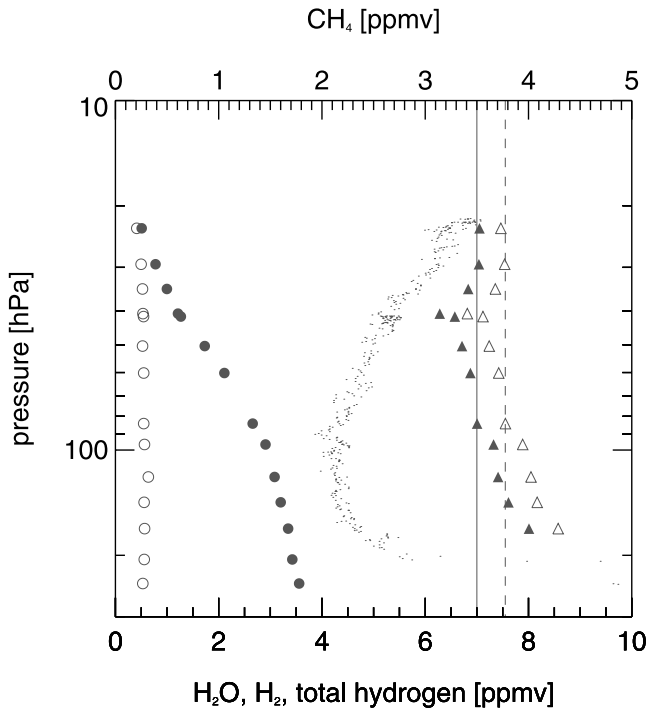

Figure 2b. Same as in Figure 2a, but for the Triple flight on 1 March 2000.

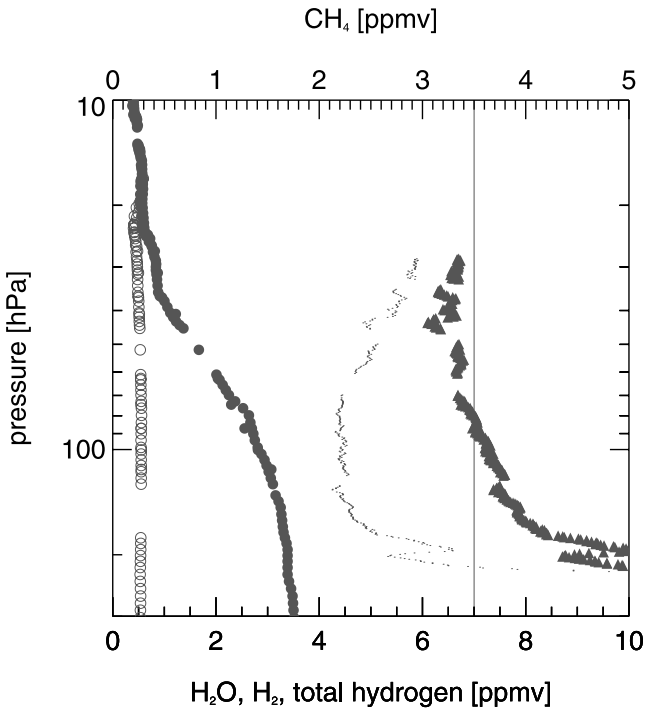

Figure 2c. Same as in Figure 2a, but for the "NOAA" and OMS flights on 5 March 2000.

of the dehydration layer seems to range down to slightly lower altitudes (>50 hPa) than for 27 January (≈45 hPa) reflecting the influence of subsidence of vortex air over this period. This effect is difficult to quantify owing to the sparse data frequency of the tracer measurements. On 5 March (Figure 2c), dehydration could also be identified around 60 hPa, however, it is not significant due to instrumental uncertainties on this flight. The reduction of $2{\cdot}CH_4 + H_2O$ also becomes obvious from a comparison of previous data listed in Table 1 and Figures 2a–2c. Above and below the dehydrated layer, $2{\cdot}CH_4 + H_2O$ is approximately 7.0 ppmv as observed in earlier measurements of the Triple payload. The total hydrogen profiles (i.e., including the H_2 measurement) show the same structure as those of $2{\cdot}CH_4 + H_2O$. Thus the observations can not be explained by chemical repartitioning amongst the hydrogen species.

[15] The H_2O profile of the LMD hygrometer launched on 19 January (Figure 1) is taken from the first ascent of the payload. During the following descent, H_2O mixing ratios agreed within 0.15 ppmv with the ascent data. In a layer between 30 and 40 hPa, H_2O data are lower by approximately 0.4 ppmv than for an assumed "smooth" profile. Unfortunately, no additional tracer measurements were obtained on this payload. Therefore a hypothetical variability due to dynamics can not be excluded. However, the observations are very similar to those of the other flights and could thus also reflect dehydration of the probed air masses.

2.3. Temperatures

[16] The measured temperatures along the balloon trajectories were generally low for all flights with minimum values in the altitude range where dehydrated layers were observed (Figure 3). On 19 January and 27 January, they were around 190 K at 40–30 hPa. Minimum values on 1 March were 192 K at 70–40 hPa, and those on 5 March were 193 K at 70–50 hPa. These temperatures are 3–5 degrees above ice saturation conditions for these altitudes and the observed water vapor mixing ratios.

[17] On both flight days in January the history of the probed air masses is comparable. First, significant stratospheric mountain wave activity occurred at the Scandinavian mountain ridge westwards of the balloon observations, that is, a few 100 km upwind. For 27 January, a vertical cross section of the temperature field along the main balloon flight using the Pennsylvania State University/National Center for Atmospheric Research mesoscale model MM5 [*Dudhia*, 1993; *Grell et al.*, 1994], operated during SOLVE/THESEO-2000 by Deutsche Luft- und Raumfahrt Oberpfaffenhofen [*Dörnbrack et al.*, 1999], is given in Figure 4a. Based on these mesoscale simulations, backtrajectories for the air masses probed by the balloon show that in the critical altitude region the air was exposed to temperatures of 189–185 K and has thus suffered ice saturation just a few hours before the measurements. Second, 10-day backward isentropic trajectories show that these air parcels experienced synoptic scale temperatures close to or even below the ice frost point for about 2 days. Figure 4b displays the temperature along backward trajectories for 27 January, based on the UK Meteorological Office (UKMO) analysis. From 500 to 550 K, temperatures were approximately 188 K, that is, corresponding to 5.0–5.5 ppmv H_2O saturation mixing ratio, for at least 70 hours several days prior to the balloon observations. A similar situation was present for the 19 January measurement.

[18] For both flight days in March the temperature history of the probed air masses was different, that is, the air was

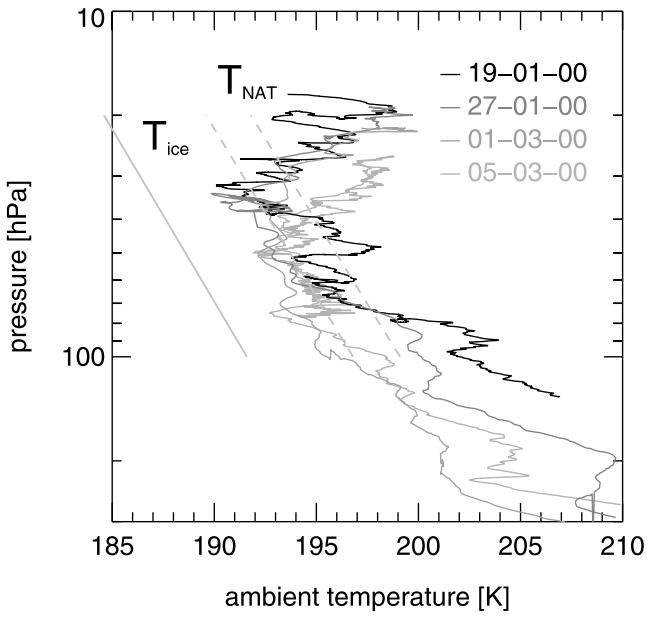

Figure 3. Temperature profiles measured during the balloon flights on 19 January, 27 January (Triple), 1 March, and 5 March 2000. Threshold temperatures for the existence of ice and NAT are indicated by gray lines. They are calculated for a smoothed January H_2O profile in Figure 1 and for HNO_3 mixing ratios of 2 and 10 ppbv, respectively. See color version of this figure at back of this issue.

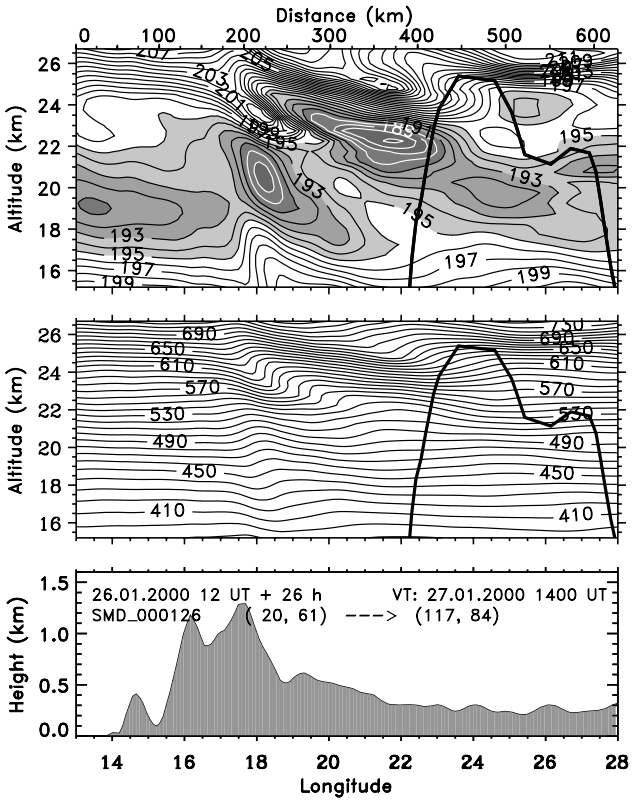

Figure 4a. Curtain files of temperature and potential temperature calculated with the MM5 mesoscale model for 27 January 2000, 1400 UT. The thick, solid line indicates the Triple balloon trajectory. (bottom) The orographic section in northern Scandinavia along which the simulations are performed.

not recently exposed to temperatures below the frost point. For example, the mesoscale analysis for 1 March shows an extended cold air mass with minimum temperatures at 18–20 km around 193 K (Figure 5a). Calculations showed no additional cooling due to mountain wave activity so that a dehydration shortly before the observation can be excluded. Also temperatures along 10-day backward trajectories did not drop below 192 K for this event (Figure 5b). A similar situation applies for the observations on 5 March.

2.4. Particle Measurements

[19] On 27 January, the DLR Falcon aircraft with an aerosol lidar tracked the balloon flight path. A diminishing mountain wave PSC was observed (Figure 6). Westward of the balloon launching site (upstream), the cloud signal from 20 to 21 km was strongly depolarizing, indicating the existence of solid ice particles in agreement with the temperature fields shown above. Based on T-matrix calculations [*Carslaw et al.*, 1998], the radii of the largest particles can be estimated to be approximately 3 μm. Downstream, where the balloon caught the cloud layer around 18 km, the particles were smaller and mainly liquid. In this layer and in a layer around 21 km, particles as large as 1 μm in radius were also observed by an optical particle counter [*Deshler and Oltmans*, 1998] on board the HALOZ balloon payload launched 1 hour after Triple, as well as by the LMD particle counter on board Triple. Number concentrations ranged from 10^{-3} to 10^{-2} cm^{-3}. However, since the particle data from both payloads differed significantly between ascent and descent, the stratospheric cloud situation downstream of the northern Scandinavian mountain ridge was rather inhomogeneous and variable for this day.

[20] On 19 January, data from backscatter sondes, optical particle counters, and the aerosol composition mass spec-

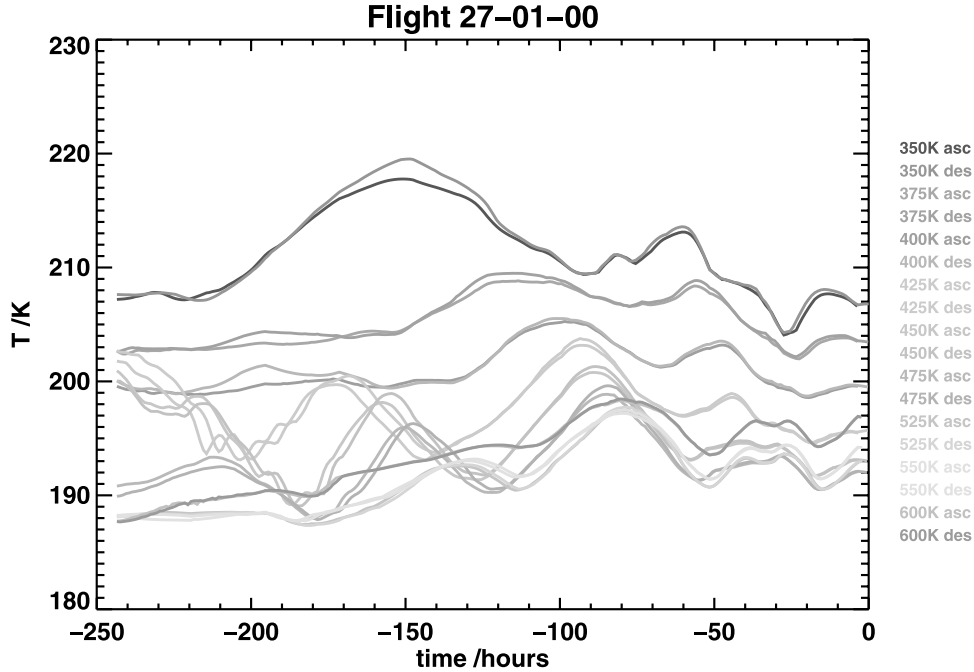

Figure 4b. Temperatures along 10-day backward isentropic trajectories ending at the trajectory of the Triple flight on 27 January 2000, based on UKMO analysis. See color version of this figure at back of this issue.

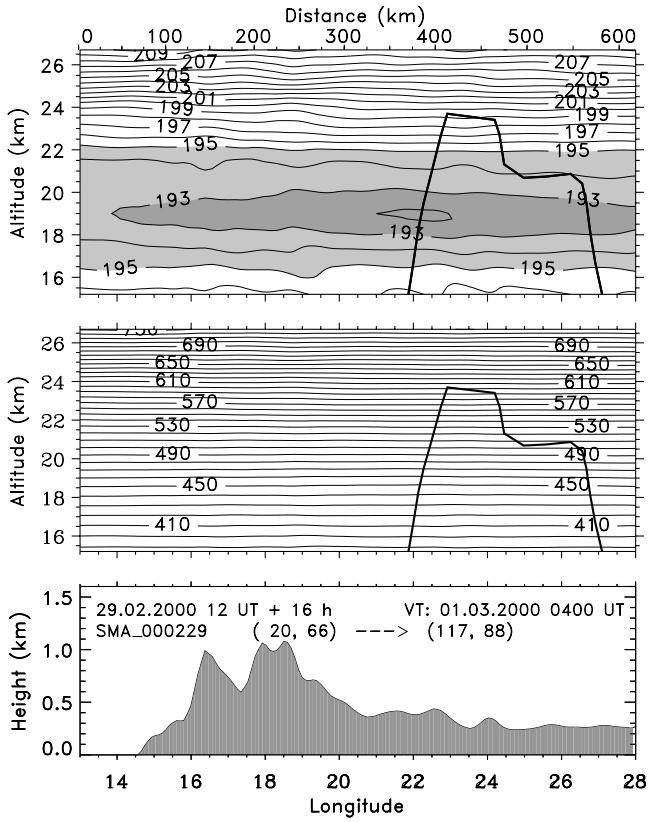

Figure 5a. Curtain files of temperature and potential temperature as in Figure 4a, but for 1 March 2000, 0400 UT.

trometer (ACMS) [*Schreiner et al.*, 1999] on the PSC analysis gondola indicated layers of solid nitric acid containing particles of up to 2–3 μm radius with number concentrations of 10^{-3} to 10^{-2} cm^{-3} at altitudes between 475 and 550 K, observed at temperatures between the threshold for the existence of nitric acid trihydrate, T_{NAT}, and 3 K below T_{NAT} (Figure 3).

[21] For 1 March, since the data of the LABS backscatter sonde on board the Triple payload above 70 hPa were affected by solar stray light, only upper limits of the backscatter ratios can be evaluated. They exclude the existence of larger ice particles, while smaller particles might have been present but not necessarily.

3. Discussion

[22] In a climatological comparison, temperatures of this winter were very low over long periods and large areas of a stable polar vortex [e.g., *Manney and Sabutis*, 2000]. In January they were lowest and comparable to those of the years 1994/1995 and 1995/1996 when dehydration events have been reported. Consequently, synoptic scale regions with the potential for PSC formation occurred over a long period of this winter. Based on 6-hourly European Centre for Medium-Range Weather Forecasts (ECMWF) analyses and the classification derived by *Dörnbrack et al.* [2001], significant mesoscale stratospheric mountain wave activity occurred in about 25% of all analyses dates during the period from January until March 2000. The adiabatic cooling in these waves decreased the temperature locally below the ice frost point above and in the lee of the Scandinavian mountain ridge.

[23] The observed reduction of H_2O by approximately 0.5 ppmv is much weaker than the corresponding phenomenon over Antarctica. This Arctic dehydration was observed at

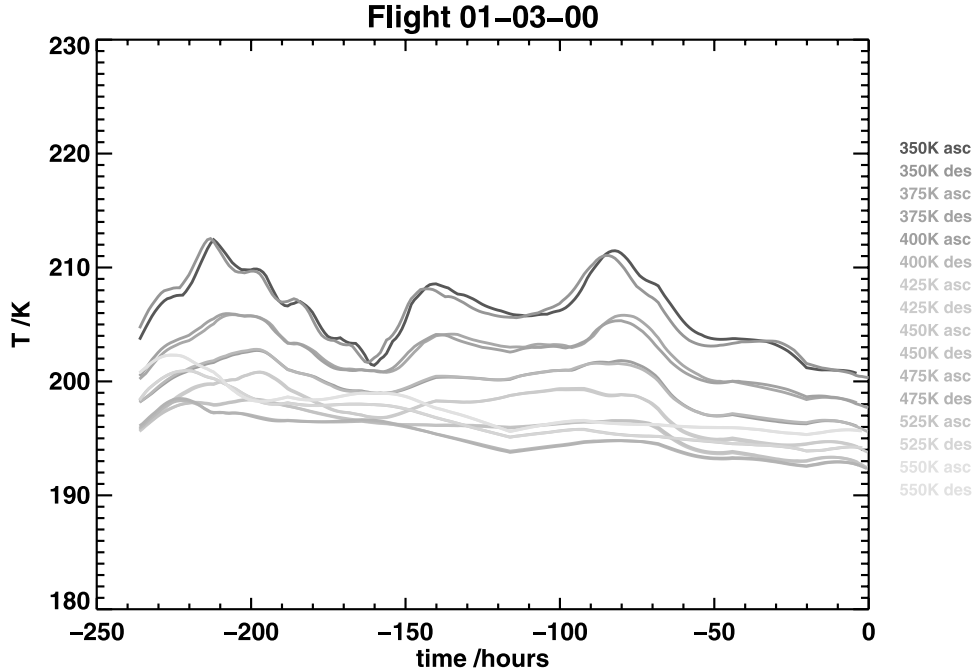

Figure 5b. Temperatures along 10-day backward isentropic trajectories ending at the trajectory of the Triple flight on 1 March 2000, based on UKMO analysis. See color version of this figure at back of this issue.

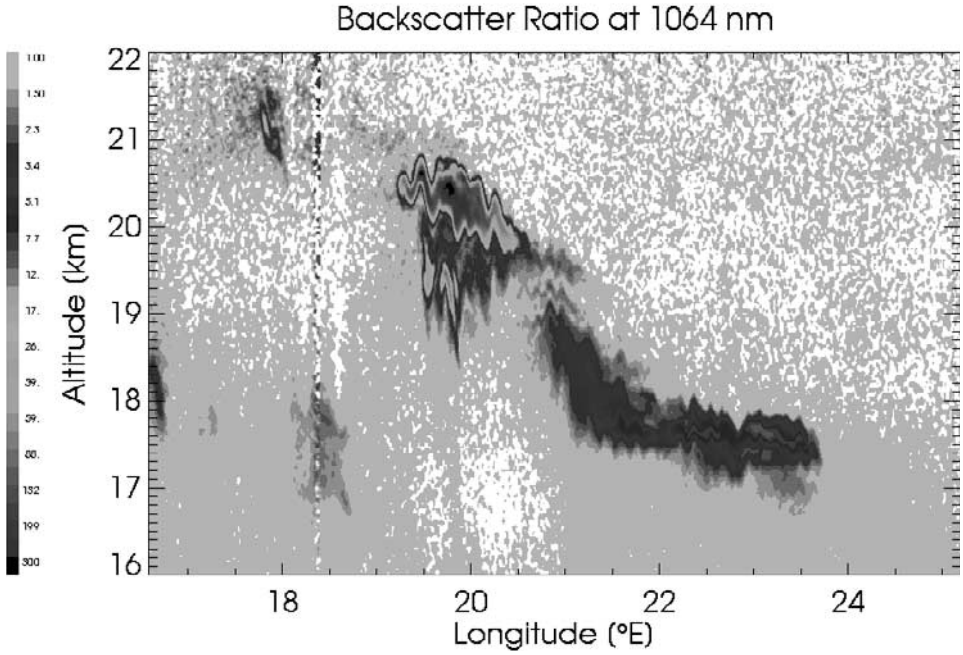

Figure 6. Lidar measurements of aerosol backscatter ratio at 1064 nm along the wind flow at PSC level measured from the Falcon aircraft on 27 January 2000. The backscatter ratio, defined as the ratio of the total backscatter coefficient (particles and molecules) to the molecular backscatter coefficient, is given in logarithmic scaling. See color version of this figure at back of this issue.

altitudes above previous Antarctic measurements, and at or above previous Arctic dehydration measurements. Measurements from the ER-2 during SOLVE indicate a weak dehydration at its highest flight altitudes at 20–21 km, in particular on 27 January, in coincidence with our balloon measurements [*Herman et al.*, 2002]. So far, only *Vömel et al.* [1997] found a dehydrated air mass at a similar height range in the Arctic. The observations by *Fahey et al.* [1990], *Hintsa et al.* [1998], *Ovarlez and Ovarlez* [1995], and *Stowasser et al.* [1999] indicated dehydration events below 20 km.

[24] Dehydration was observed in all balloon observations between January and early March which reached the altitude region around 40 hPa, regardless of the temperature observed during the flights or even the temperature history along the backward trajectories. This is clear evidence that the observed dehydration was not a local or occasional phenomenon but rather a widespread feature of the Arctic polar vortex in early 2000. Nevertheless, this does not rule out lee waves as an explanation from the beginning, as formation of ice particles occurs in many air masses as they pass though lee wave regions with sufficiently low temperatures, making dehydration a synoptic scale feature. As discussed below, the problem with lee wave clouds is rather whether particles live long enough and are large enough to sediment.

[25] During SOLVE/THESEO-2000 the altitude range of low temperatures and ice clouds observed in the lee of the Scandinavian mountain ridge coincides with that of the dehydrated layers. The calculated temperature reduction in these regions is sufficient to saturate the air, and the corresponding saturation mixing ratio is approximately 5 ppmv in accordance with the measurements. On the other hand, the growth rate and subsequent subsidence rates for ice particles in mountain waves is not sufficient to dry a layer of more than 1 km thickness, as observed, within a few hours only, which is the typical residence time of an air parcel in a mountain wave. As indicated by the airborne lidar measurements on this day, the particles in the ice clouds grew up to sizes of approximately 3 μm radii, corresponding to a sedimentation rate of the order of 5 m h^{-1} [e.g., *Müller and Peter*, 1992]. Therefore this process can only be considered if several mesoscale events accumulate or the mountain waves were stationary for longer periods. The high frequency of such events over the Scandinavian mountain ridge and over Greenland during this winter could generally have contributed to the observed dehydration.

[26] The air parcels of the January observation were already exposed to temperatures at the ice frost point several days before in synoptic-scale cold regions. There temperatures of approximately 188 K also correspond to a saturation mixing ratio of 5 ppmv as measured in the dehydrated air masses over Scandinavia and are thus consistent with the observed relatively moderate dehydration by only 0.5 ppmv compared to Antarctic observations. Under these conditions, particles can grow up to sizes of 10 μm radii within a few hours [e.g., *Peter et al.*, 1994]. Since the air was exposed to these temperatures for a duration of at least 50 hours, the particles have likely grown to such sizes. Sedimentation of these particles occurs at rates of the order of 100 m h^{-1} in the lower and middle stratosphere. Thus the time is sufficient to dehydrate a layer of 1–2 km thickness.

[27] The finding of a moderate dehydration at these altitudes is also calculated by the NASA Langley Research

Center (LaRC) Lagrangian chemical transport model: *Pierce et al.* [2002] simulate the large-scale evolution of the Arctic vortex during the 1999/2000 winter. The result is a H_2O loss of 0.6 ppmv at 500 K until March that the authors attribute to late December and January ice clouds.

[28] Simultaneous particle measurements do not indicate the presence of larger ice crystals in the dehydrated air masses themselves, and temperatures were not low enough for the existence of ice clouds. Since FISH measured total water (27 January and 1 March), it can be excluded that the reduction in the measured water was due to a reduction in the gas phase alone. But also the data of the frost point hygrometers which measure only the gas phase show an irreversible dehydration, since the mass of the particles in the air masses does not account for the missing water.

[29] For 19 and 27 January, however, smaller particles were present in these layers. *Voigt et al.* [2000] observed a PSC event under similar conditions on 25 January, when such particles were identified as solid nitric acid trihydrate (NAT). Also on 19 January, the ACMS measured nitric acid and water in PSC particles with radii of a few microns, and in both cases the temperatures were below the NAT existence threshold. As indicated by the 10-day backward trajectory analysis and/or the mesoscale model results, the PSC particles in these measurements may have frozen earlier into ice crystals and then remained in the solid state until observation. The presence of dehydration is strong evidence for preceding formation of ice particles in these air masses. These ice crystals, whether originating from the synoptic cold region or from the lee waves, might have served as the nucleus for the formation of the smaller solid particles. The mechanism that aerosol droplets have to be supercooled below the ice frost point before they crystallize has been postulated in the past [e.g., *Koop et al.*, 1995]. Thus the observations are consistent with these theories and do not require additional freezing processes above the frost point as discussed by *Drdla et al.* [2002].

4. Summary and Conclusions

[30] During the SOLVE/THESEO-2000 winter, layers whose water vapor content was reduced by approximately 0.5 ppmv were observed on five balloon flights. For the January measurements, trajectory calculations and mesoscale modeling show that these dehydrated air masses were recently exposed to low temperatures corresponding to saturation mixing ratios which are consistent with the observed ones. Since the March measurements can not be traced back to similar recent cold events, water vapor must have been removed in an earlier stage of the winter. From these findings we conclude that removal of water was irreversible over larger areas of the polar vortex and persistent during this winter. The degree of dehydration, however, is less severe than observed over Antarctica. Further, the phenomenon was apparent above 20 km, that is, at higher altitudes than the layers of strongest dehydration in the austral winter.

[31] The most likely process that might have caused the observed phenomena is ice particle growth and subsequent sedimentation in synoptic-scale cold areas over a few days. Such cold areas with temperatures below ice saturation were identified for the winter 1999/2000 during January [*Manney and Sabutis*, 2000], which can be directly linked with our observations. Further, ice clouds were observed several times in the lee of the Scandinavian mountains and over Greenland during this winter. During periods of mountain wave activity up to 20% of the total stratospheric mass flux above the northern part of the Scandinavian mountain ridge is processed by mesoscale mountain waves even when the synoptic-scale temperatures are above the ice frost point [*Dörnbrack et al.*, 2001]. Though the timescales of processing air in these events is much shorter, we can not exclude an additional impact by these lee wave clouds on the removal of water vapor.

[32] The consequences of dehydration for the chemical processing of vortex air masses are still uncertain. In Antarctica, the frequent occurrence of ice clouds is believed to provide the basis for the observed massive denitrification, though the hemispheric difference suggests that some Antarctic dehydration may have occurred without denitrification. In the Arctic, intense denitrification is observed without intense dehydration [e.g., *Fahey et al.*, 1990; *Waibel et al.*, 1999]. The observation of large nitric acid trihydrate particles during the 1999/2000 winter provides evidence that particles other than ice may become large enough to remove HNO_3 by sedimentation [*Fahey et al.*, 2001]. Thus the key role played by ice particles may not be sedimentary removal of HNO_3 directly, but rather the initiation of nitric acid trihydrate particles (small ones were indeed found in some of our observations, see previous section): *Waibel et al.* [1999] developed a scenario assuming NAT particles to nucleate on ice particles falling from above, and the ice to be released upon warming above the frost point at lower altitudes. Such a mechanism can result in a moderate dehydration at higher altitudes where ice particles are created, and in denitrification also in the layers below. Thus ice might have initiated the nucleation of some of the large HNO_3-containing particles during the winter 1999/2000 [*Fahey et al.*, 2001], though it seems to be unlikely that it is the dominant source of these clouds in the period until March [*Carslaw et al.*, 2002]. The detection of widespread dehydration in a layer at 20–22 km during the SOLVE/THESEO-2000 winter proves that ice particles were formed in early stages of the winter. It provides one of the fundamental parameters and verifiable criteria for the different scenarios which are developed to explain the particle observations and related chemical processing in the Arctic polar vortex.

[33] **Acknowledgments.** We would like to thank the teams of CNES, ESRANGE, and NSBF to launch the balloons under difficult conditions in the Arctic. The effort and assistance of Jochen Barthels, Jürgen Beuermann, Erich Klein, Fred L. Moore, Christian Poss, Holger Röppischer, Bärbel Vogel, and Thomas Wetter to carry out the balloon measurements and data analysis are gratefully acknowledged. Part of the experimental activities was supported by the European Commission, DG XII, under various contracts within the THESEO program, and by the U.S. National Science Foundation.

References

Adriani, A., et al., A new joint balloon-borne experiment to study polar stratospheric clouds: Laser backscatter sonde and optical particle counter, in *Proceedings of the XVIII Quadrennial Ozone Symposium, L'Aquila 1996*, edited by R. D. Bojkov and G. Visconti, pp. 879–882, International Ozone Commission, 1998.

Carslaw, K. S., et al., Particle microphysics and chemistry in remotely observed mountain polar stratospheric clouds, *J. Geophys. Res.*, *103*, 5785–5796, 1998.

Carslaw, K. S., et al., A vortex-scale simulation of the growth and sedimentation of large nitric acid hydrate particles, *J. Geophys. Res.*, *107*, 10.1029/2001JD000467, in press, 2002.

de la Noë, J., et al., Water vapour distribution inside and outside the polar vortex during THESEO, Proc. 5th Europ. Workshop on Stratospheric Ozone, St. Jean de Luz, France, *EU Air Pollu. Res. Rep.*, *73*, 558–561, 1999.

Deshler, T., and S. J. Oltmans, Vertical profiles of volcanic aerosol and polar stratospheric clouds above Kiruna, Sweden: Winters 1993 and 1995, *J. Atmos. Chem.*, *30*, 11–23, 1998.

Dörnbrack, A., M. Leutbecher, R. Kivi, and E. Kyrö, Mountain wave induced record low stratospheric temperatures above northern Scandinavia, *Tellus Ser A.*, *51*, 951–963, 1999.

Dörnbrack, A., M. Leutbecher, J. Reichardt, A. Behrendt, K.-P. Müller, and G. Baumgarten, Relevance of mountain wave cooling for the formation of polar stratospheric clouds over Scandinavia: Mesoscale dynamics and observations for January 1997, *J. Geophys. Res.*, *106*, 1569–1581, 2001.

Drdla, K., M. R. Schoeberl, and E. V. Browell, Microphysical modeling of the 1999/2000 Arctic winter, 1, Polar stratospheric clouds, denitrification, and dehydration, *J. Geophys. Res.*, *107*, 10.1029/2001JD000782, in press, 2002.

Dudhia, J., A nonhydrostatic version of the Penn State NCAR Mesoscale Model: Validation tests and simulation of an Atlantic cyclone and cold front, *Mon. Weather Rev.*, *121*, 1493–1513, 1993.

Engel, A., et al., The total hydrogen budget in the Arctic winter stratosphere during the European Arctic Stratospheric Ozone Experiment, *J. Geophys. Res.*, *101*, 14,495–14,503, 1996.

Fahey, D. W., K. K. Kelly, S. R. Kawa, A. F. Tuck, M. Loewenstein, K. R. Chan, and L. E. Heidt, Observations of denitrification and dehydration in the winter polar stratosphere, *Nature*, *344*, 321–324, 1990.

Fahey, D. W., et al., The detection of large HNO_3-containing particles in the winter Arctic stratosphere, *Science*, *291*, 1026–1031, 2001.

Grell, G. A., J. Dudhia, and D. R. Stauffer, A description of the fifth-generation Penn State/NCAR mesoscale model (MM5), *NCAR Tech. Note 398*, p. 121, Nat. Cent. for Atmos. Res., Boulder, Colo., 1994.

Herman, R. L., et al., Hydration, dehydration, and the total hydrogen budget of the 1999–2000 winter Arctic stratosphere, *J. Geophys. Res.*, *107*, doi:10.1029/2001JD001257, in press, 2002.

Hintsa, E., et al., Dehydration and denitrification in the Arctic polar vortex during the 1995–1996 winter, *Geophys. Res. Lett.*, *25*, 501–504, 1998.

Kelly, K. K., et al., Dehydration in the lower Antarctic stratosphere during late winter and early spring, 1987, *J. Geophys. Res.*, *94*, 11,317–11,357, 1989.

Kelly, K. K., et al., A comparison of ER-2 measurements of stratospheric water vapor between the 1987 Antarctic and 1989 Arctic airborne missions, *Geophys. Res. Lett.*, *17*, 465–468, 1990.

Koop, T., U. M. Biermann, W. Raber, B. P. Luo, P. J. Crutzen, and T. Peter, Do stratospheric aerosol droplets freeze above the ice frost point?, *Geophys. Res. Lett.*, *22*, 917–920, 1995.

Manney, G. L., and J. L. Sabutis, Development of the polar vortex in the 1999–2000 Arctic winter stratosphere, *Geophys. Res. Lett.*, *27*, 2589–2592, 2000.

Müller, R., and T. Peter, The numerical modeling of the sedimentation of polar stratospheric cloud particles, *Ber. Bunsenges. Phys. Chem.*, *96*, 353–361, 1992.

Nedoluha, G., et al., POAM III measurements of dehydration in the Antarctic lower stratosphere, *Geophys. Res. Lett.*, *27*, 1683–1686, 2000.

Oltmans, S. J., Measurements of water vapor in the stratosphere with a frost point hygrometer, in *Measurement and Control in Science and Industry*, *Proc. 1985 International Symposium on Moisture and Humidity*, pp. 251–258, Instrum. Soc. of Am., Washington, D. C., 1985.

Ovarlez, J., and H. Ovarlez, Stratospheric water vapor content evolution during EASOE, *Geophys. Res. Lett.*, *21*, 1235–1238, 1994.

Ovarlez, J., and H. Ovarlez, Water vapour and aerosol measurements during SESAME and the observation of low water vapour content layers, *Air Pollut. Rep. 56*, pp. 205–208, Polar Stratospheric Ozone Comm. of Eur. Commun., Luxemberg, 1995.

Pawson, S., and B. Naujokat, The cold winters of the middle 1990s in the northern lower stratosphere, *J. Geophys. Res.*, *104*, 14,209–14,222, 1999.

Peter, T., R. Müller, P. Crutzen, and T. Deshler, The lifetime of leewave-induced ice particles in the Arctic stratosphere; II, Stabilization due to NAT-coating, *Geophys. Res. Lett.*, *21*, 1331–1334, 1994.

Pierce, R. B., et al., Large-scale chemical evolution of the Arctic vortex during the 1999–2000 winter: HALOE/POAM-3 Lagrangian photochemical modeling for the SAGE III ozone loss and validation experiment (SOLVE) campaign, *J. Geophys. Res.*, *107*, 10.1029/2001JD001063, in press, 2002.

Randel, W. J., et al., Seasonal cycles and QBO variations in stratospheric CH_4 and H_2O observed in UARS HALOE data, *J. Atmos. Sci.*, *55*, 163–185, 1998.

Ray, E. A., et al., Transport into the Northern Hemisphere lowermost stratosphere revealed by in situ tracer measurements, *J. Geophys. Res.*, *104*, 26,565–26,580, 1999.

Schiller, C., T. Deshler, and T. Peter, Contamination-induced particle production during balloon flights: Origin for unexpected ice particle observations in the Arctic?, *Geophys. Res. Lett.*, *28*, 10.1029/2001GL013295, 2001.

Schmidt, U., and A. Khedim, In situ measurements of carbon dioxide in the winter Arctic vortex and at midlatitudes: An indicator of the "age" of stratospheric air, *Geophys. Res. Lett.*, *18*, 763–766, 1991.

Schmidt, U., et al., Intercomparison of balloon-borne cryogenic whole air samplers during the Map/Globus 1983 Campaign, *Planet. Space Sci.*, *35*, 647–656, 1987.

Schreiner, J., C. Voigt, A. Kohlmann, F. Arnold, K. Mauersberger, and N. Larsen, Chemical analysis of polar stratospheric cloud particles, *Science*, *283*, 968–970, 1999.

Stowasser, M., et al., Simultaneous measurements of HDO, H_2O, and CH_4 with MIPAS-B: Hydrogen budget and indication of dehydration inside the polar vortex, *J. Geophys. Res.*, *104*, 19,213–19,225, 1999.

Vogel, B., F. Stroh, J.-U. Grooß, R. Müller, D. S. McKenna, M. Müller, T. Deshler, D. Toohey, G. Toon, and J. Karhu, Vertical profiles of activate ClO and ozone loss in the Arctic vortex in January and March 2000: In situ observations and model simulations, *J. Geophys. Res.*, *107*, doi:10.1029/2002JD002564, in press, 2002.

Voigt, C., et al., Nitric acid trihydrate (NAT) in polar stratospheric clouds, *Science*, *290*, 1756–1758, 2002.

Vömel, H., et al., The evolution of the dehydration in the Antarctic stratospheric vortex, *J. Geophys. Res.*, *100*, 13,919–13,926, 1995.

Vömel, H., et al., Dehydration and sedimentation of ice particles in the Arctic stratospheric vortex, *Geophys. Res. Lett.*, *24*, 795–798, 1997.

Waibel, A. E., et al., Arctic ozone loss due to denitrification, *Science*, *283*, 2064–2068, 1999.

Zöger, M., et al., Fast in situ stratospheric hygrometers: A new family of balloon-borne and airborne Lyman α photofragment fluorescence hygrometers, *J. Geophys. Res.*, *104*, 1807–1816, 1999.

R. Bauer, C. Schiller, and F. Stroh, Forschungszentrum Jülich, ICG-I, 52425 Jülich, Germany. (r.bauer@fz-juelich.de; c.schiller@fz-juelich.de; f.stroh@fz-juelich.de)

F. Cairo, Instituto di Fisica dell'Atmosfera-Consiglio Nazionale delle Ricerche, via Fosso del Cavaliere, 100, 00133 Rome, Italy. (cairo@ifa.rm.cnr.it)

T. Deshler, Department of Atmospheric Sciences, University of Wyoming, P.O. Box 3038 University Station, Laramie, WY 82071, USA. (deshler@uwyo.edu)

A. Dörnbrack, H. Flentje, and C. Voigt, Deutsches Zentrum für Luft-und Raumfahrt, Institut für Physik der Atmosphäre, P.O. Box 1116, 82234 Wessling, Germany. (andreas.doernbrack@dlr.de; harald.flentje@dlr.de; christiane.voigt@dlr.de)

J. Elkins, S. Oltmans, and H. Vömel, Climate Monitoring and Diagnostics Laboratory, NOAA, 325 Broadway, Boulder, CO 80303, USA. (Jelkins@cmdl.noaa.gov; soltmans@cmdl.noaa.gov; hvoemel@cmdl.noaa.gov)

A. Engel and M. Müller, J. W. Goethe Universität Frankfurt, Institut für Meteorologie und Geophysik, P.O. Box 111932, 60054 Frankfurt, Germany. (an.engel@meteor.uni-frankfurt.de)

N. Larsen, Danish Meteorological Institute, Lyngbyvej 100, 2100 Copenhagen, Denmark. (nl@dmi.dk)

I. Levin, Institut für Umweltphysik, Universität Heidelberg, Im Neuenheimer Feld 229, 69120 Heidelberg, Germany.

H. Ovarlez and J. Ovarlez, Laboratoire de Météorologie Dynamique, CNRS, Ecole Polytechnique, 91128 Palaiseau cedex, France. (joelle.ovarlez@polytechnique.fr)

J. Schreiner, Max-Planck-Institut für Kernphysik, P.O. Box 103980, 69029 Heidelberg, Germany.

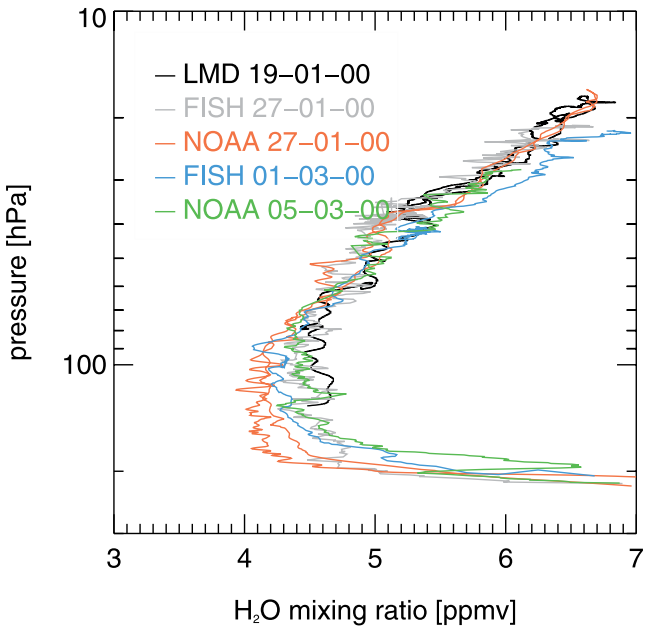

Figure 1. H_2O profiles measured during SOLVE/THESEO-2000 on 19 January, 27 January, 1 March, and 5 March 2000.

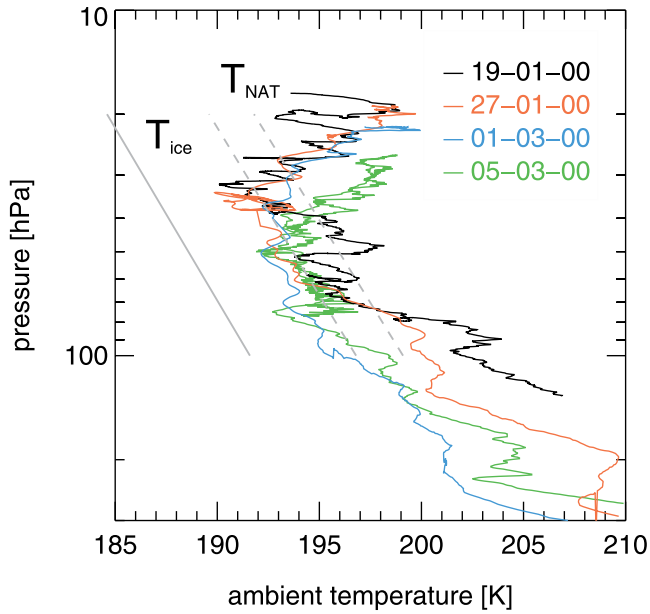

Figure 3. Temperature profiles measured during the balloon flights on 19 January, 27 January (Triple), 1 March, and 5 March 2000. Threshold temperatures for the existence of ice and NAT are indicated by gray lines. They are calculated for a smoothed January H_2O profile in Figure 1 and for HNO_3 mixing ratios of 2 and 10 ppbv, respectively.

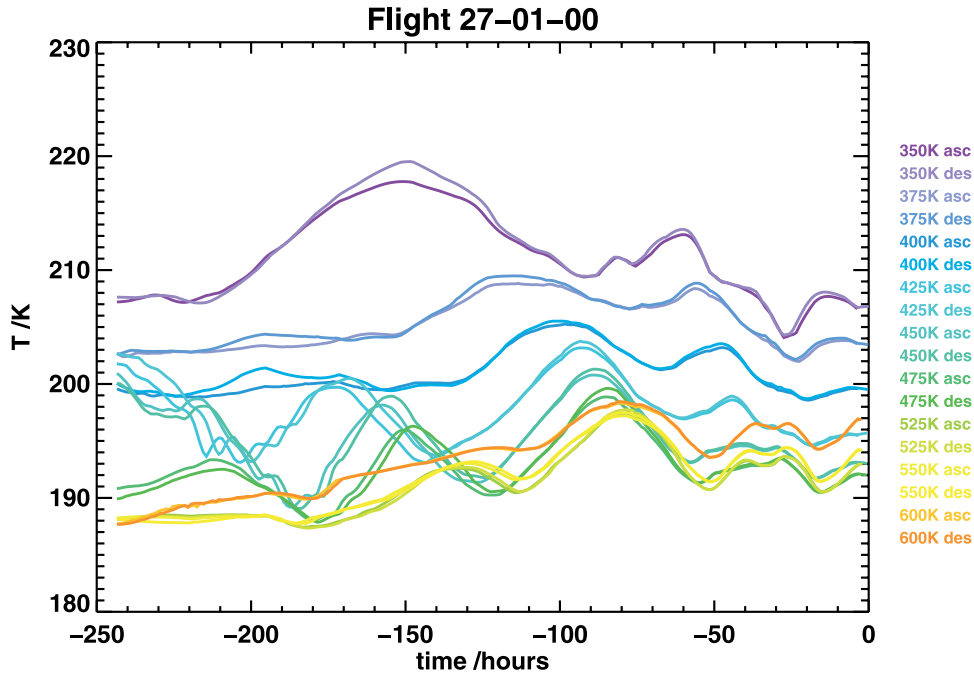

Figure 4b. Temperatures along 10-day backward isentropic trajectories ending at the trajectory of the Triple flight on 27 January 2000, based on UKMO analysis.

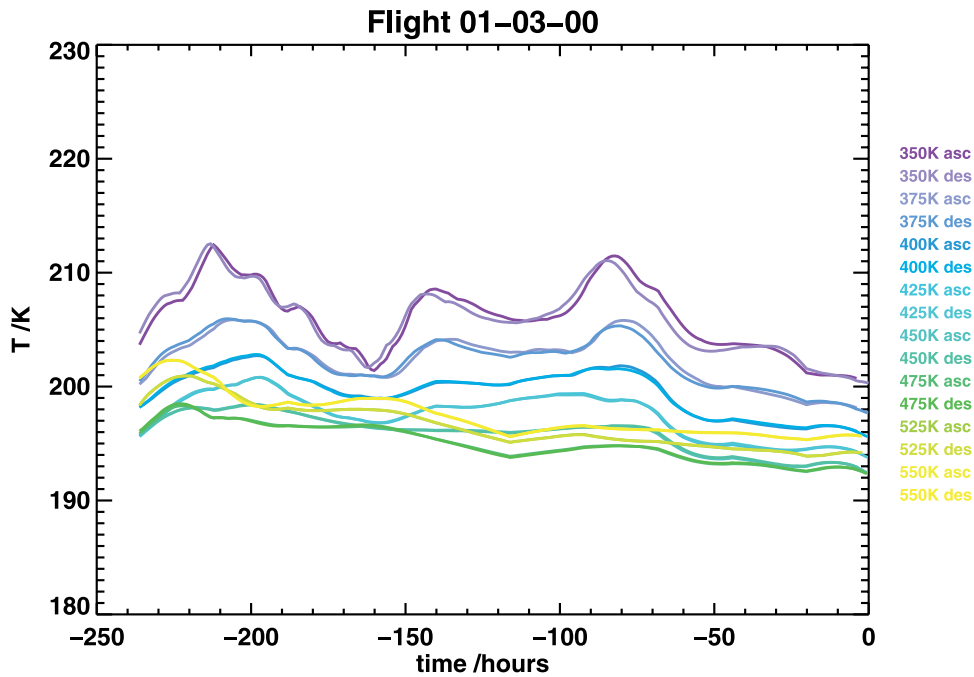

Figure 5b. Temperatures along 10-day backward isentropic trajectories ending at the trajectory of the Triple flight on 1 March 2000, based on UKMO analysis.

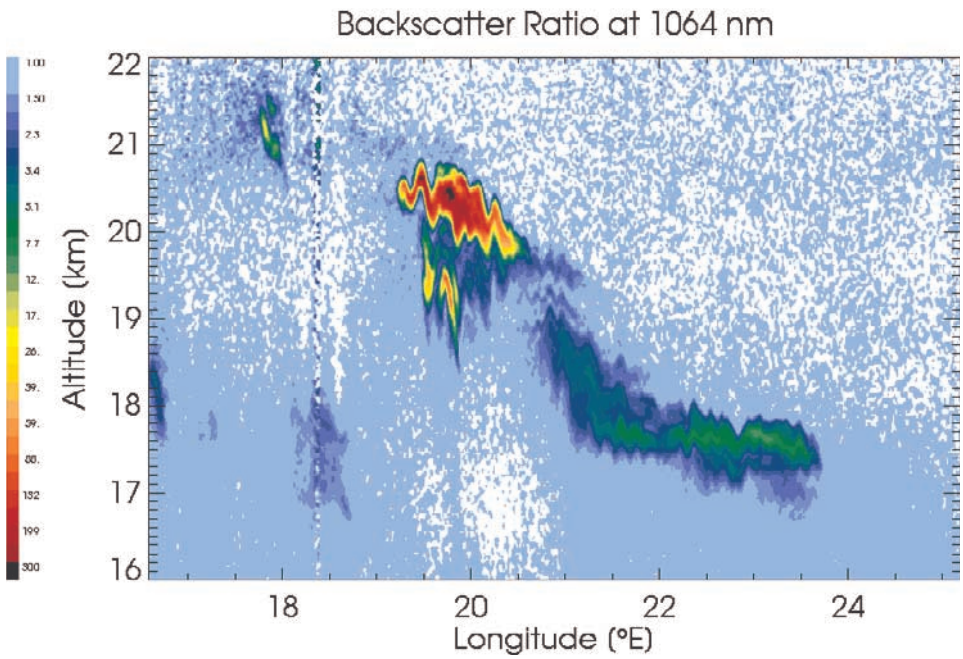

Figure 6. Lidar measurements of aerosol backscatter ratio at 1064 nm along the wind flow at PSC level measured from the Falcon aircraft on 27 January 2000. The backscatter ratio, defined as the ratio of the total backscatter coefficient (particles and molecules) to the molecular backscatter coefficient, is given in logarithmic scaling.